

Quantum critical point in the Sc-doped itinerant antiferromagnet TiAu

E. Svanidze,^{1,*} T. Besara,² J. K. Wang,¹ D. Geiger,³ L. Prochaska,³ J. M. Santiago,¹ J. W. Lynn,⁴
S. Paschen,³ T. Siegrist,² and E. Morosan¹

¹*Department of Physics and Astronomy, Rice University, Houston, Texas 77005, USA*

²*National High Magnetic Field Laboratory, Florida State University, Tallahassee, Florida 32306, USA*

³*Institute of Solid State Physics, TU Wien, 1040 Vienna, Austria*

⁴*NIST Center for Neutron Research, National Institute of Standards and Technology, Gaithersburg, Maryland 20899, USA*

(Received 27 May 2016; revised manuscript received 18 October 2016; published 14 June 2017)

We present an experimental realization of a quantum critical point in an itinerant antiferromagnet composed of nonmagnetic constituents, TiAu. By partially substituting Ti with Sc in $\text{Ti}_{1-x}\text{Sc}_x\text{Au}$, a doping amount of $x_c = 0.13 \pm 0.01$ induces a quantum critical point with minimal disorder effects. The accompanying non-Fermi liquid behavior is observed in both the resistivity $\rho \propto T$ and specific heat $C_p/T \propto -\ln T$, characteristic of a two-dimensional antiferromagnet. The quantum critical point is accompanied by an enhancement of the spin fluctuations, as indicated by the diverging Sommerfeld coefficient γ at $x = x_c$.

DOI: [10.1103/PhysRevB.95.220405](https://doi.org/10.1103/PhysRevB.95.220405)

Quantum criticality is one of the central tenants of condensed matter physics. Intense research on quantum critical systems has brought several questions to the forefront: What are the differences between ferromagnetic (FM) and antiferromagnetic (AFM) quantum critical fluctuations? Is the quantum critical behavior analogous in *local* and *itinerant* moment systems? The former question is motivated by the many known AFM systems with quantum critical points (QCPs), with correspondingly fewer known FM analogs. The latter question has numerous ramifications, considering the complexity of the phenomena accompanying QCPs in both *d*- and *f*-electron systems: unconventional superconductivity [1–4], non-Fermi liquid (NFL) [5–8] and heavy fermion (HF) behavior [7,9–12]. In this Rapid Communication we report a QCP in the first itinerant antiferromagnetic metal (IAFM) without magnetic constituents, TiAu [13]. By comparison with the only two other itinerant magnets with no magnetic elements, ZrZn_2 [14] and $\text{Sc}_{3,1}\text{In}$ [15], both ferromagnets, we will articulate the differences and similarities stemming from the two kinds of magnetic order.

The *d*-electron (transition metal) systems showing quantum criticality are noticeably fewer than the *f*-electron (rare earth) ones, with remarkably few (only three) transition metal itinerant magnets (IMs) with *no magnetic elements*: the itinerant ferromagnets (IFMs) ZrZn_2 [14], $\text{Sc}_{3,1}\text{In}$ [15], and the IAFM TiAu [13]. Surprising similarities and substantive differences exist between the FM and AFM ordered states, in *both* local and itinerant moment systems: (i) pressure [16] and doping [17] both suppress the FM order in ZrZn_2 , but have opposite effects in the IFM $\text{Sc}_{3,1}\text{In}$ [18,19]; (ii) NFL behavior accompanies the QCP in the doped FMs, the *d*-electron $\text{Sc}_{3,1}\text{In}$ [19], and *f*-electron HF URu_2Si_2 [20], with non-mean-field scaling in both compounds contrasting the mean-field and Fermi liquid (FL) behavior in the IFM ZrZn_2 [17]; (iii) modest pressure increases the magnetic ordering temperature in both the IAFM TiAu [21] and the IFM $\text{Sc}_{3,1}\text{In}$ [18]. Here we present experimental data compatible with a two-dimensional (2D) AFM QCP in the *d*-electron system $\text{Ti}_{1-x}\text{Sc}_x\text{Au}$, with a critical

composition $x_c = 0.13 \pm 0.01$. The evidence for 2D quantum fluctuations stems from the continuous suppression of T_N with x in $\text{Ti}_{1-x}\text{Sc}_x\text{Au}$, accompanied by both a logarithmically divergent Sommerfeld coefficient $\gamma(T)$ and a linear electrical resistivity $\rho(T)$ close to the QCP. Minimal disorder effects can be deduced from the electrical transport behavior, and the relative elastic and inelastic contributions to $\rho(T)$ at and away from the QCP.

Recently, we reported orthorhombic TiAu as the first IAFM metal with no magnetic constituents [13]. The AFM order in TiAu develops below 36 K, and T_N is slightly enhanced by the application of pressure [21], in a manner reminiscent of the IFM $\text{Sc}_{3,1}\text{In}$ [18]. Since Ti bands contribute the most to the density of states (DOS) at the Fermi energy E_F [13], doping on the Ti sublattice is a promising avenue for experimentally suppressing T_N toward zero. In this Rapid Communication, Sc was chosen as a dopant in $\text{Ti}_{1-x}\text{Sc}_x\text{Au}$ because of its similarity in ionic radius to Ti ($r[\text{Sc}^{3+}] = 0.75 \text{ \AA}$ and $r[\text{Ti}^{4+}] = 0.61 \text{ \AA}$) [22]. Magnetization, specific heat, and electrical resistivity data reveal a continuous suppression of the AFM order in $\text{Ti}_{1-x}\text{Sc}_x\text{Au}$ as a function of x . Quantum criticality is accompanied by linear electrical resistivity ρ and diverging Sommerfeld coefficient γ , both consistent with a 2D NFL. This is an observation of a 2D AFM QCP in a transition metal system.

Crystallographically, orthorhombic TiAu can be viewed as a three-dimensional (3D) structure [Fig. 1(b) in Ref. [13]], even though the interplanar bond lengths are only slightly larger than the intraplanar Ti-Au distances. Even though doping TiAu with the slightly larger Sc ion results in a modest unit-cell volume V increase of about 4% between the $x = 0$ and 0.25 samples [diamonds, Fig. S1(a) [23]], this is due mostly to an increase in the intraplanar lattice parameter b (circles), with the interplanar spacing c (triangles) virtually independent of x . It would appear that, crystallographically, TiAu remains nearly 3D, even though it will be shown below that the quantum critical behavior induced by Sc doping points toward quasi-2D spin fluctuations. Such dimensional discrepancy has been observed in the HF compound $\text{CeCu}_{6-x}\text{Au}_x$ [24], with a possible explanation attributed to a dimensional crossover in the vicinity of an AFM QCP [25].

*Present address: Max Planck Institute for Chemical Physics.

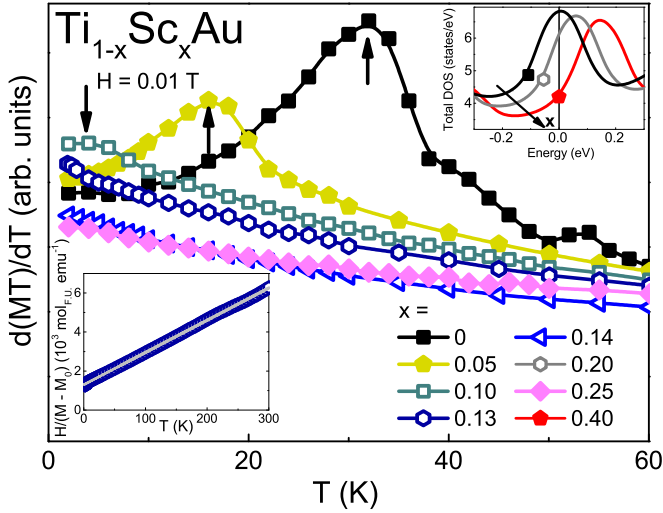


FIG. 1. The Néel temperature T_N (indicated by arrows) for $\text{Ti}_{1-x}\text{Sc}_x\text{Au}$, determined from the peak in $d(MT)/dT$. Bottom inset: Inverse susceptibility $H/(M - M_0)$ (symbols) along with the Curie-Weiss-like fit (line) for $x = 0.13$ (1 emu = 10 A cm⁻²). Top inset: The density of states calculated for $x = 0, 0.2$, and 0.4 .

In $\text{Ti}_{1-x}\text{Sc}_x\text{Au}$, the suppression of the magnetic order with increasing x is first signaled by the magnetic susceptibility. In Fig. 1, a cusp in $d(MT)/dT$, reminiscent of the Néel temperature T_N signature in local moment antiferromagnets [26], moves down in T with increasing x and is suppressed to below 0.4 K for $x \geq 0.13$. The band structure calculations reinforce this point, as a peak in the DOS (top inset, Fig. 1) occurs at the Fermi energy for $x = 0$, and moves away from E_F with doping. The continuous decrease of T_N with doping x , similar to what has been seen in the AFM $\text{Cr}_{1-x}\text{V}_x$ [27], is consistent with a second order AFM QCP. At high temperatures ($T > T_N$), the $H = 0.01$ T magnetic susceptibility M/H exhibits Curie-Weiss-like behavior, rendering the inverse susceptibility $H/(M - M_0)$ linear (bottom inset, Fig. 1), where M_0 is a temperature-independent susceptibility contribution. The linear fits in the paramagnetic (PM) state (with an example shown as a solid line for $x = 0.13$) indicate that the PM moment $\mu_{\text{PM}} \sim 0.8\mu_B$ f.u.⁻¹ remains nearly unaffected by the increasing x even beyond the AFM state. This was also the case in the IFM $(\text{Sc}_{1-x}\text{Lu}_x)_{3.1}\text{In}$ [19]. The Curie-Weiss-like behavior has been observed in the doped IFMs ZrZn_2 and $\text{Sc}_{3.1}\text{In}$ [17,19], but not in the archetypical 3D IAFM Cr, in which the magnetization increased on warming [28]. The magnetic susceptibility of Cr is in disagreement with the self-consistent renormalization (SCR) theory, which predicts Curie-Weiss-like behavior for both the 2D [29] and 3D [30] antiferromagnets.

The differences between doped TiAu and Cr deepen in the electrical transport properties. The resistivity of TiAu [13] decreases below T_N , a likely indication that the loss of spin-disorder scattering overcomes the expected enhancement of the resistivity due to the partial gapping of the Fermi surface with the AFM order. By contrast, the partial gapping of the Fermi surface upon magnetic ordering [31] is dominant in Cr, resulting in a resistivity increase below T_N . A more significant distinction between TiAu and Cr occurs in their

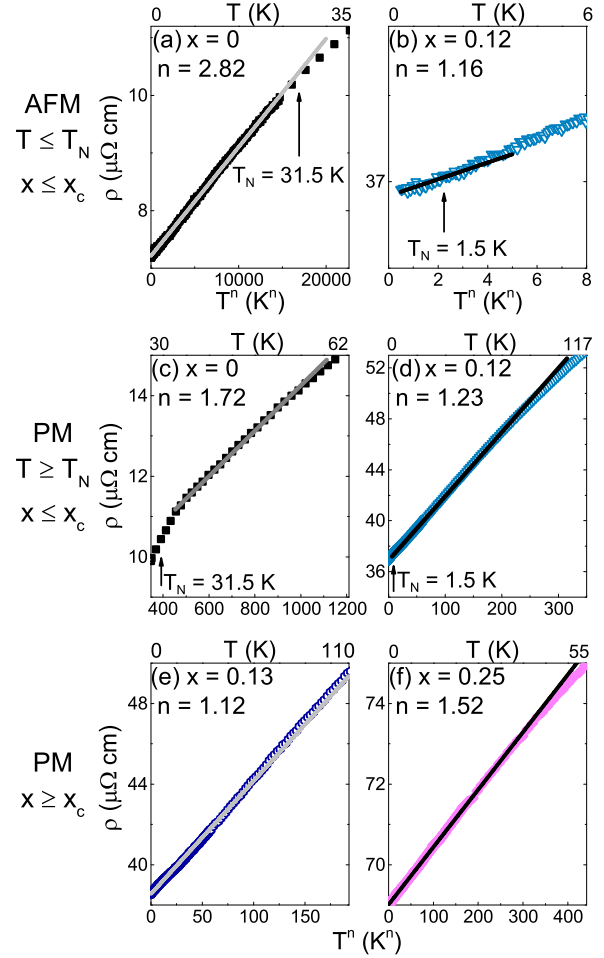


FIG. 2. Resistivity $\rho(T) = \rho_0 + A_n T^n$ as a function of temperature T^n for $\text{Ti}_{1-x}\text{Sc}_x\text{Au}$ for the AFM state (top row) (a),(b) $x \leq x_c$, $T \leq T_N$; and the PM state (middle row) (c),(d) $x \leq x_c$, $T \geq T_N$; (bottom row) (e),(f) $x \geq x_c$. (a)–(d) The ordering temperature T_N is marked by vertical arrows.

respective quantum critical regimes: while magnon scattering results in $\rho = \rho_0 + A_n T^n$, $n = 3$ [32] for both TiAu and Cr, doping affects the resistivity exponent $n(x; T)$ differently. In Cr, $n(x; T)$ remains constant even across the QCP [27], but in $\text{Ti}_{1-x}\text{Sc}_x\text{Au}$ $n \approx 1$ close to the QCP at $x_c \approx 0.13$. These $n(x; T)$ values are best reflected in the ρ vs T^n plots, shown in Fig. 2: the top row panels (a) and (b) depict the $\rho \sim T^n$ behavior in the AFM state ($T \leq T_N$; $x \leq x_c$). The two bottom rows correspond to the PM state: for panels (c) and (d) $x \leq x_c$ and $T > T_N$, while for panels (e) and (f) $x \geq x_c$.

In the AFM state, n decreases from 3 to 1, while in the PM state, n has a nonmonotonic dependence on x . A drastic change in the resistivity slope at T_N for $x = 0$ [Fig. 2(c)] marks the crossover from the magnon-dominated transport with $n \approx 3$, to the FL behavior in the PM state $n \approx 2$ for $T > T_N$. With increasing x up to 0.08 [Figs. S3(g)–S3(i) [23]], n remains close to the FL value in the PM state.

Upon approaching the QCP from both below ($x \leq 0.13$) and above ($x > 0.13$) [Figs. S3(j) and S3(k)–S3(o) [23]], n decreases toward 1 in the quantum critical region, corroborating the NFL scenario close to the QCP, which is also evident from the specific heat data shown in Fig. 3. In the quantum critical

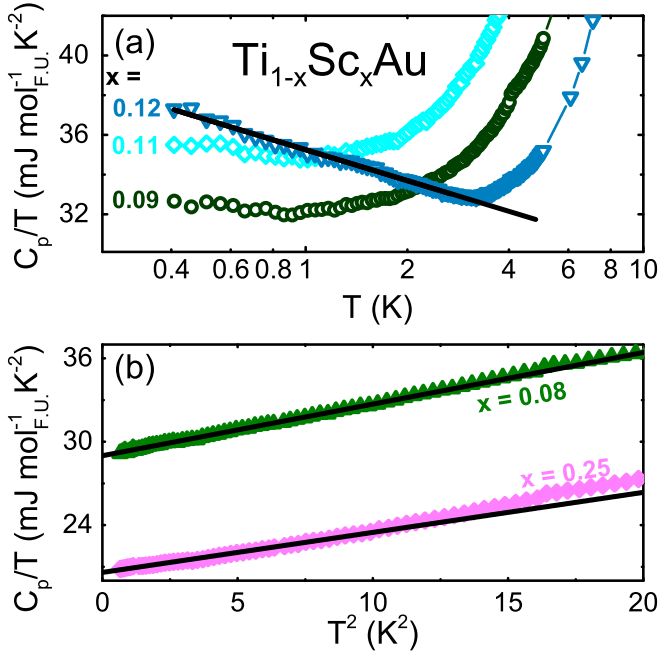


FIG. 3. (a) Specific heat C_p/T vs $\ln T$ for $\text{Ti}_{1-x}\text{Sc}_x\text{Au}$ with $0.09 \leq x \leq 0.12$. (b) Specific heat $C_p/T \propto T^2$ for $x = 0.08$ and $x = 0.25$.

region $0.09 \leq x \leq 0.20$, C_p/T increases on cooling, and it has a logarithmic divergence $\gamma = C_p/T \propto \ln T$, a signature of NFL behavior close to a QCP. The logarithmic C_p/T persists over a decade in temperature for $x \sim x_c$ [Fig. 3(a)]. Away from the QCP [Fig. 3(b)], linear C_p/T vs T^2 indicates FL behavior. The resulting γ values increase from $16 \text{ mJ mol}^{-1} \text{K}^{-2}$ for $x = 0$ to $30 \text{ mJ mol}^{-1} \text{K}^{-2}$ upon approaching x_c . The x dependence of the Sommerfeld coefficient γ is summarized in Fig. S2(c) [23]: the full symbols are determined from the $T = 0$ intercepts of C_p/T vs T^2 in Fig. S2(a) [23]; the open symbols correspond to the $T = 0.4 \text{ K}$ C_p/T values (Fig. S2 [23]), which represent underestimates of the $\gamma(T = 0)$ values due to the divergent specific heat in the NFL regime. With this in mind, the strong enhancement of $\gamma(x)$ at x_c [Fig. S2(c) [23]] actually signals the divergence of $\gamma(x)$ on one or both sides of the QCP (gray line), akin to the behavior noted for $\text{Cr}_{1-x}\text{V}_x$ [33]. This strongly suggests a spin fluctuation contribution to the γ_{SF} [34]. According to the SCR theory for antiferromagnets [30], $T_N \propto (2I\chi_s - 1)^{2/3}$ and $\gamma_{\text{SF}} \propto (2I\chi_s - 1)^{1/2}$, where I is the exchange interaction and χ_s is the staggered susceptibility. This yields that the spin fluctuation contribution to γ_{SF} increases as $T_N^{3/4}$. Indeed, assuming γ_{SF} is proportional to the amount of dopant x , this power-law dependence is reflected in the T_N^δ vs x plot in Fig. 4 (triangles), where $\delta \approx (3 \pm 0.3)/4$. Such power-law dependence attests both to the presence of strong spin fluctuations and the validity of the SCR theory in $\text{Ti}_{1-x}\text{Sc}_x\text{Au}$ [35]. Remarkably, the lower limit for this exponent, $\delta \approx (3 - 0.3)/4 = 2/3$, coincides with that predicted for the quantum critical suppression of the ordering temperature with pressure [36]. This prediction is in disagreement with several doping- or pressure-induced AFM QCPs, for which $\delta = 1$ [27,37,38] or $\delta = 1/2$ [39]. The origin of this disagreement is an important open problem [36], with

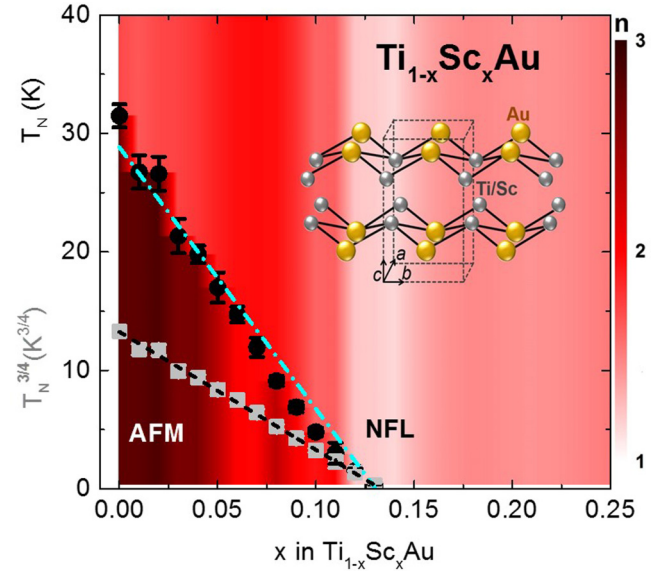


FIG. 4. $T_N - x$ phase diagram (symbols) with the contour plot rendering the resistivity exponent $n(x; T)$. Inset: $\text{Ti}_{1-x}\text{Sc}_x\text{Au}$ crystal structure.

the $\text{Ti}_{1-x}\text{Sc}_x\text{Au}$ system providing an experimental realization of the predicted $\delta > 1$ value.

The continuous suppression of the Néel temperature with x is shown in Fig. 4 for $\text{Ti}_{1-x}\text{Sc}_x\text{Au}$ (circles), together with a contour plot of n in $\rho(T) = \rho_0 + A_n T^n$. The experimental data for $\text{Ti}_{1-x}\text{Sc}_x\text{Au}$ point to a QCP at $x_c = 0.13 \pm 0.01$, with associated 2D quantum fluctuations. The evidence for a QCP comes from (i) the second order transition as $T_N \rightarrow 0$, suggested by the continuous decrease of T_N with x , (ii) a power-law temperature dependence of the resistivity $\rho = \rho_0 + A_n T^n$ (Fig. 2) with $n \approx 1$, and (iii) a diverging Sommerfeld coefficient γ [Fig. S2(c) [23]] when $T_N \rightarrow 0$. Away from the QCP, the specific heat becomes FL-like $C_p = \gamma T + \beta T^3$ [Fig. 3(b)]. The resistivity exponent $n(x; T)$ (contour plot in Fig. 4) has a minimum around $n = 1$ at the critical composition. Below the QCP $n(x; T)$ increases with increasing $|x - x_c|$, up to $n = 3$ and $n = 2$ in the AFM and PM states, respectively, while above x_c $n(x; T)$ increases from 1 to 1.5 for the composition range under study. Resistivity exponent values $n < 1.5$ close to a QCP have been attributed to reduced dimensionality [3], with $n = 1.5$ and 1 expected, respectively, for 3D and 2D AFM QCPs [40]. This suggests that the quantum critical fluctuations in $\text{Ti}_{1-x}\text{Sc}_x\text{Au}$ are more 2D than 3D [24,41]. In IAFMs, the deviations from FL behavior have also been discussed in terms of resistivity contributions due to quantum critical AFM spin fluctuations and disorder scattering [42–44]. However, the role of disorder in quantum critical systems is not easily resolved, with the difficulty inherent in the convoluted effects of doping (charge doping together with some atomic disorder, chemical pressure, etc.). For example, in the case of V-doped Cr, small ρ_0 ($\rho_0 \approx 5 \mu\Omega \text{ cm}$) indicated likely negligible disorder effects [27], as was the case in the IFMs $(\text{Sc}_{1-x}\text{Lu}_x)_{3.1}\text{In}$ ($20 \mu\Omega \text{ cm}$) [19] and ZrZn_2 ($5 \mu\Omega \text{ cm}$) [45]. In the IAFM $\text{Ti}_{1-x}\text{Sc}_x\text{Au}$, $\rho_0 \approx 30 \mu\Omega \text{ cm}$ at x_c , which is to be expected for good metals in polycrystalline form. The residual resistivity ratios (RRR) $= \rho(300 \text{ K})/\rho_0 \sim 2$ for $\text{Ti}_{1-x}\text{Sc}_x\text{Au}$ are also

comparable with those of other polycrystalline IM systems, e.g., $(\text{Sc}_{1-x}\text{Lu}_x)_3\text{In}$ ($\text{RRR} < 4$ [19]). These are all indications that disorder scattering represents a small contribution to the resistivity in $\text{Ti}_{1-x}\text{Sc}_x\text{Au}$. A further argument that discredits dominant disorder effects in $\text{Ti}_{1-x}\text{Sc}_x\text{Au}$ is the resistivity change $\Delta\rho$ in the linear range compared to the residual (defect) resistivity contribution ρ_0 . Strong disorder effects are typically signaled by $\Delta\rho \ll \rho_0$. For all of the $\text{Ti}_{1-x}\text{Sc}_x\text{Au}$ samples, $\Delta\rho$ and ρ_0 are of the same order of magnitude (Fig. 2). The issue of clean versus dirty limit in doped TiAu still remains, with the added complications that these samples are polycrystalline. Single crystals will allow us to perform a detailed study of the electrical transport in this system, and this is an ongoing effort in our laboratory.

Given the small disorder effects in $\text{Ti}_{1-x}\text{Sc}_x\text{Au}$, a comparison with the SCR theory of spin fluctuations is justified: While HF QCPs are strongly affected by disorder [42], incorporating these effects into the SCR theory of spin fluctuations for IMs has not yet been accomplished [46]. The description of the behavior close to a QCP for d -electron systems was established for both FM [35] and AFM materials [40]. However, while these predictions were validated experimentally in a number of FM QCPs [17,19,32,37,44,47–50], the limited number of d -electron antiferromagnets hinders an analogous analysis in AFM systems [6]. Among d -electron magnets, an AFM QCP has so far only been reached in V_{2-y}O_3 [31,51] and Cr [27,33,39,52–55]. In vanadium oxide, the QCP is accompanied by an insulator-to-metal transition [51] and the AFM order arises from local rather than itinerant moments. Cr, on the other hand, is the archetypical 3D IAFM metal for which charge carriers are lost as they become localized upon cooling through the Néel temperature T_N . Interestingly enough, no signatures of quantum criticality in resistivity data were observed in Cr with either doping or pressure, making it impossible to compare the resistivity exponents with those expected from the SCR theory [46]. While it was suggested that a 2D AFM metal should exhibit a continuous second order QPT [56], experimentally this has not yet been realized until the current doped TiAu, perhaps explaining why the characteristics of metallic 2D AFM QPTs remained one of the pressing questions from both theoretical and experimental viewpoints [6]. The

results in $\text{Ti}_{1-x}\text{Sc}_x\text{Au}$ ought to be compared with the behavior of $4f$ QCPs. Doped CeCu_6 provides the closest HF analog, in light of its potential 2D AFM QCP and dimensional crossover: In $\text{CeCu}_{6-x}\text{Au}_x$, NFL close to, and FL behavior away from the QCP, were evident from both specific heat and resistivity data [5]. Even though the compound has a 3D orthorhombic crystal structure, the quantum critical regime of $\text{CeCu}_{6-x}\text{Au}_x$ was consistent with a 2D AFM QCP [46], suggesting the possibility of a dimensional crossover close to the QCP [25]. A similar dimensional crossover likely occurs in TiAu upon doping.

In this work, the suppression of the AFM order in the IAFM TiAu to a QCP was possible via partial substitution of Ti with Sc in $\text{Ti}_{1-x}\text{Sc}_x\text{Au}$, with a critical composition $x_c = 0.13 \pm 0.01$. Moreover, the suppression of the AFM transition with Sc doping was also confirmed by band structure calculations, in which a gradual shift of the peak in the DOS at E_F was observed. This is consistent with a decreasing number of d electrons upon substituting Ti with Sc. Neutron diffraction measurements also indicate the absence of magnetic order close to x_c [57]. Although 2D AFM QCPs have been reported for $4f$ -electron systems such as YbRh_2Si_2 [7], CeIn_3 [10], and CeRhIn_5 [11], this behavior in $\text{Ti}_{1-x}\text{Sc}_x\text{Au}$ is an observation in d -electron materials. Ongoing pressure experiments are expected to reveal the quantum critical scaling in the absence of doping-induced disorder, while the study of V-doped TiAu [58] will allow for a comparison between electron (V) and hole (Sc) doping effects in TiAu.

We thank Q. Si, E. Abrahams, A. Nevidomskyy, J. Analytis, V. Martelli, A. J. Millis, A. Wieteska, and P. Dai for useful discussions, and J. Aman for assistance with data fits. The work at Rice was supported by NSF DMR-1506704 (E.S., J.M.S. and E.M.). T.B. and T.S. are supported by the U.S. DOE, BES, Materials Science and Engineering Division, under award DE-SC0008832. A portion of this work was performed at the National High Magnetic Field Laboratory, which is supported by NSF Cooperative Agreement DMR-1157490 and the State of Florida. D.G., L.P., and S.P. acknowledge support by the European Research Council (ERC Advanced Researcher Grant No. 227378) and the Austrian Science Fund (FWF doctoral program W1243).

-
- [1] J. R. Jeffries, N. A. Frederick, E. D. Bauer, H. Kimura, V. S. Zapf, K. D. Hof, T. A. Sayles, and M. B. Maple, *Phys. Rev. B* **72**, 024551 (2005).
- [2] R. A. Cooper, Y. Wang, B. Vignolle, O. J. Lipscombe, S. M. Hayden, Y. Tanabe, T. Adachi, Y. Koike, M. Nohara, H. Takagi *et al.*, *Science* **323**, 603 (2009).
- [3] N. D. Mathur, F. M. Grosche, S. R. Julian, I. R. Walker, D. M. Freye, R. K. W. Haselwimmer, and G. G. Lonzarich, *Nature (London)* **394**, 39 (1998).
- [4] S. Saxena, P. Agarwal, K. Ahilan, F. Grosche, R. Haselwimmer, M. Steiner, E. Pugh, I. Walker, S. Julian, P. Monthoux *et al.*, *Nature (London)* **406**, 587 (2000).
- [5] H. v. Löhneysen, T. Pietrus, G. Portisch, H. G. Schlager, A. Schröder, M. Sieck, and T. Trappmann, *Phys. Rev. Lett.* **72**, 3262 (1994).
- [6] H. v. Löhneysen, A. Rosch, M. Vojta, and P. Wölfle, *Rev. Mod. Phys.* **79**, 1015 (2007).
- [7] P. Gegenwart, J. Custers, C. Geibel, K. Neumaier, T. Tayama, K. Tenya, O. Trovarelli, and F. Steglich, *Phys. Rev. Lett.* **89**, 056402 (2002).
- [8] E. D. Bauer, V. S. Zapf, P. C. Ho, N. P. Butch, E. J. Freeman, C. Sirvent, and M. B. Maple, *Phys. Rev. Lett.* **94**, 046401 (2005).
- [9] A. Schröder, G. Aeppli, R. Coldea, M. Adams, O. Stockert, H. Löhneysen, E. Bucher, R. Ramazashvili, and P. Coleman, *Nature (London)* **407**, 351 (2000).
- [10] G. Knebel, D. Braithwaite, P. C. Canfield, G. Lapertot, and J. Flouquet, *Phys. Rev. B* **65**, 024425 (2001).
- [11] G. Knebel, D. Aoki, J. P. Brison, and J. Flouquet, *J. Phys. Soc. Jpn.* **77**, 114704 (2008).

- [12] J. Custers, K. A. Lorenzer, M. Müller, A. Prokofiev, A. Sidorenko, H. Winkler, A. M. Strydom, Y. Shimura, T. Sakakibara, R. Yu *et al.*, *Nat. Mater.* **11**, 189 (2012).
- [13] E. Svanidze, J. K. Wang, T. Besara, L. Liu, Q. Huang, T. Siegrist, B. Frandsen, J. W. Lynn, A. H. Nevidomskyy, M. B. Gamza *et al.*, *Nat. Commun.* **6**, 7701 (2015).
- [14] B. T. Matthias and R. M. Bozorth, *Phys. Rev.* **109**, 604 (1958).
- [15] B. T. Matthias, A. M. Clogston, H. J. Williams, E. Corenzwit, and R. C. Sherwood, *Phys. Rev. Lett.* **7**, 7 (1961).
- [16] T. F. Smith, J. A. Mydosh, and E. P. Wohlfarth, *Phys. Rev. Lett.* **27**, 1732 (1971).
- [17] D. A. Sokolov, M. C. Aronson, W. Gannon, and Z. Fisk, *Phys. Rev. Lett.* **96**, 116404 (2006).
- [18] J. Grewe, J. S. Schilling, K. Ikeda, and K. A. Gschneidner, *Phys. Rev. B* **40**, 9017 (1989).
- [19] E. Svanidze, L. Liu, B. Frandsen, B. D. White, T. Besara, T. Goko, T. Medina, T. J. S. Munsie, G. M. Luke, D. Zheng, C. Q. Jin, T. Siegrist, M. B. Maple, Y. J. Uemura, and E. Morosan, *Phys. Rev. X* **5**, 011026 (2015).
- [20] N. P. Butch and M. B. Maple, *Phys. Rev. Lett.* **103**, 076404 (2009).
- [21] C. T. Wolowiec, Y. Fang, C. A. McElroy, J. R. Jeffries, R. L. Stillwell, E. Svanidze, J. M. Santiago, E. Morosan, S. T. Weir, Y. K. Vohra, and M. B. Maple, *Phys. Rev. B* **95**, 214403 (2017).
- [22] R. D. Shannon, *Acta Crystallogr.* **32**, 751 (1976).
- [23] See Supplemental Material at <http://link.aps.org/supplemental/10.1103/PhysRevB.95.220405> for structural analysis along with resistivity data and band structure calculations.
- [24] A. Rosch, A. Schroder, O. Stockert, and H. v. Löhneysen, *Phys. Rev. Lett.* **79**, 159 (1997).
- [25] M. Garst, L. Fritz, A. Rosch, and M. Vojta, *Phys. Rev. B* **78**, 235118 (2008).
- [26] M. E. Fisher, *Philos. Mag.* **7**, 1731 (1962).
- [27] A. Yeh, Y. Soh, J. Brooke, G. Aeppli, T. F. Rosenbaum, and S. M. Hayden, *Nature (London)* **419**, 459 (2002).
- [28] T. R. McGuire and C. J. Kriessman, *Phys. Rev.* **85**, 452 (1952).
- [29] A. Ishigaki and T. Moriya, *J. Phys. Soc. Jpn.* **67**, 3924 (1998).
- [30] H. Hasegawa and T. Moriya, *J. Phys. Soc. Jpn.* **36**, 1542 (1974).
- [31] W. Bao, C. Broholm, G. Aeppli, S. A. Carter, P. Dai, T. F. Rosenbaum, J. M. Honig, P. Metcalf, and S. F. Trevino, *Phys. Rev. B* **58**, 12727 (1998).
- [32] A. Ishikawa, *J. Phys. Soc. Jpn.* **51**, 441 (1982).
- [33] J. Takeuchi, H. Sasakura, and Y. Masuda, *J. Phys. Soc. Jpn.* **49**, 508 (1980).
- [34] H. Hasegawa, *J. Phys. Soc. Jpn.* **38**, 107 (1975).
- [35] T. Moriya, *Spin Fluctuations in Itinerant Electron Magnetism* (Springer-Verlag, Berlin/Heidelberg, 1985).
- [36] L. B. Ioffe and A. J. Millis, *Phys. Usp.* **41**, 595 (1998).
- [37] S. R. Julian, C. Pfleiderer, F. M. Grosche, N. D. Mathur, G. J. McMullan, A. J. Diver, I. R. Walker, and G. G. Lonzarich, *J. Phys.: Condens. Matter* **8**, 9675 (1996).
- [38] H. v. Löhneysen, *J. Phys.: Condens. Matter* **8**, 9689 (1996).
- [39] M. Lee, A. Husmann, T. F. Rosenbaum, and G. Aeppli, *Phys. Rev. Lett.* **92**, 187201 (2004).
- [40] T. Moriya and T. Takimoto, *J. Phys. Soc. Jpn.* **64**, 960 (1995).
- [41] P. Coleman and A. J. Schofield, *Nature (London)* **433**, 226 (2005).
- [42] A. Rosch, *Phys. Rev. Lett.* **82**, 4280 (1999).
- [43] C. Pfleiderer, A. Faisst, H. von Löhneysen, S. M. Hayden, and G. G. Lonzarich, *J. Magn. Magn. Mater.* **226-230**, 258 (2001).
- [44] M. Nicklas, M. Brando, G. Knebel, F. Mayr, W. Trinkl, and A. Loidl, *Phys. Rev. Lett.* **82**, 4268 (1999).
- [45] R. P. Smith, M. Sutherland, G. G. Lonzarich, S. S. Saxena, N. Kimura, S. Takashima, M. Nohara, and H. Takagi, *Nature (London)* **455**, 1220 (2008).
- [46] T. Moriya and K. Ueda, *Adv. Phys.* **49**, 555 (2000).
- [47] G. Lonzarich, *J. Magn. Magn. Mater.* **45**, 43 (1984).
- [48] Y. Ishikawa, Y. Noda, Y. J. Uemura, C. F. Majkrzak, and G. Shirane, *Phys. Rev. B* **31**, 5884 (1985).
- [49] Y. Takahashi and T. Moriya, *J. Phys. Soc. Jpn.* **54**, 1592 (1985).
- [50] C. Pfleiderer, G. J. McMullan, S. R. Julian, and G. G. Lonzarich, *Phys. Rev. B* **55**, 8330 (1997).
- [51] H. Kadowaki, K. Motoya, T. J. Sato, J. W. Lynn, J. A. Fernandez-Baca, and J. Kikuchi, *Phys. Rev. Lett.* **101**, 096406 (2008).
- [52] D. B. McWhan and T. M. Rice, *Phys. Rev. Lett.* **19**, 846 (1967).
- [53] R. Jaramillo, Y. Feng, J. C. Lang, Z. Islam, G. Srajer, P. B. Littlewood, D. B. McWhan, and T. F. Rosenbaum, *Nature (London)* **459**, 405 (2009).
- [54] R. Jaramillo, Y. Feng, J. Wang, and T. F. Rosenbaum, *Proc. Natl. Acad. Sci. USA* **107**, 13631 (2010).
- [55] D. A. Sokolov, M. C. Aronson, L. Wu, Y. Zhu, C. Nelson, J. F. Mansfield, K. Sun, R. Erwin, J. W. Lynn, M. Lumsden *et al.*, *Phys. Rev. B* **90**, 035139 (2014).
- [56] A. Abanov, A. V. Chubukov, and A. M. Finkel'stein, *Europhys. Lett.* **54**, 488 (2001).
- [57] E. Svanidze, J. W. Lynn, P. Dai, and E. Morosan (unpublished).
- [58] J. Santiago, E. Svanidze, T. Besara, T. Siegrist, and E. Morosan (unpublished).